Delft University of Technology

2D steady-state RANS simulations of the Aerospatiale A-Airfoil

Delft University of Technology, Delft, South Holland, 2628 CD

Changkyu Park* 4646061

Malte Wegener* 4672194

Submission Date: Monday 16th November, 2020

Course: AE4202

Contents

*Graduate Student, Faculty of Aerospace Engineering, Delft University of Technology, Kluyverweg 1, 2629 HS Delft

1. Pre-processing

1.1. Mesh

The flow field around the airfoil was partitioned into into different blocks in order to allow for fine control over the element size in different parts of the domain while aiding the formulation of orthogonal elements as much as possible. This blocking of the geometry was based on the degree of cell orthogonality that is achievable while maintaining a smooth inlet boundary.. The mesh topology is a C-grid comprised of hexahedral elements, with a single element in the z direction. The blocking can be seen in Figure 1.

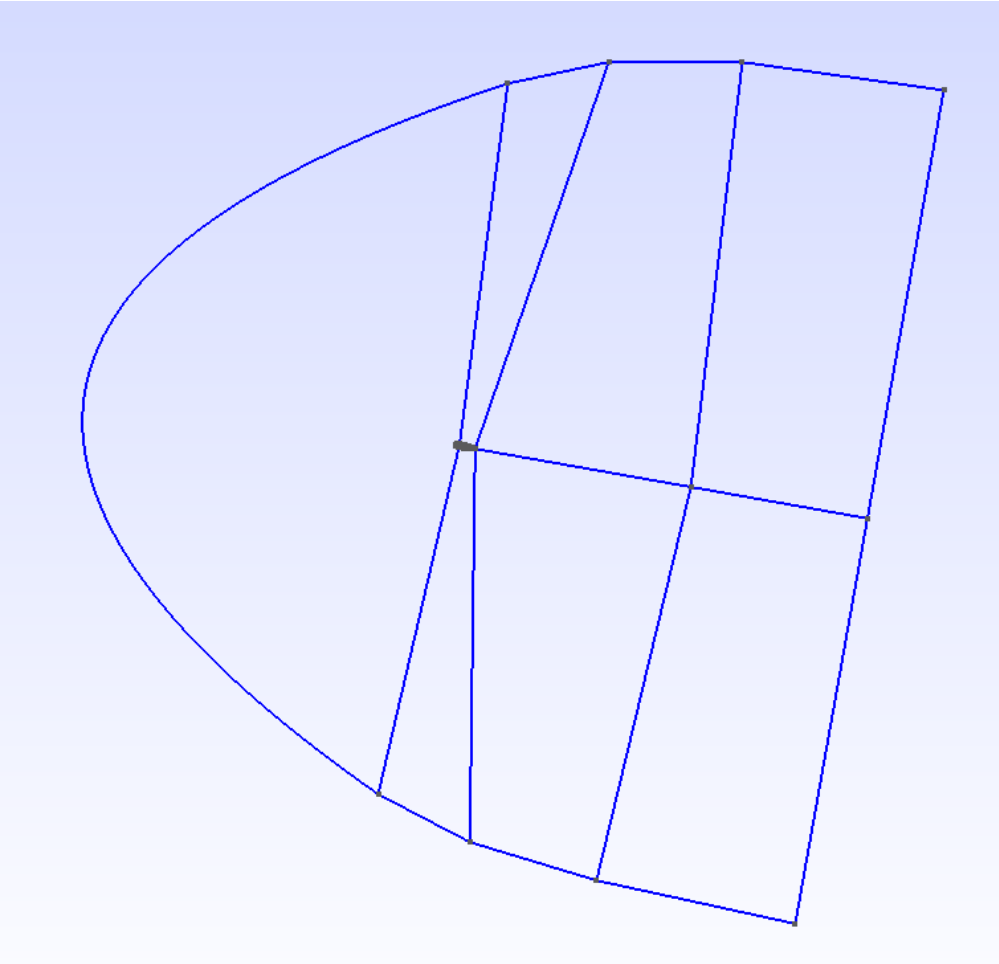

Fig. 1 Mesh blocking

A coarse mesh with 21286 hexahedra was generated for an initial simulation run. In order to partially resolve the boundary layer, the first cell size close to the airfoil was chosen to be 1 mm. Mesh quality parameters for this mesh were obtained from OpenFOAM utilities. The maximum aspect ratio of cells was 13, which is commendable for a mesh. The mesh is close to orthogonal with an average angle of 11 degrees from orthogonality. From a visual analysis the progression of element sizes looks smooth over the whole domain. This mesh is visualised in Figure 2.

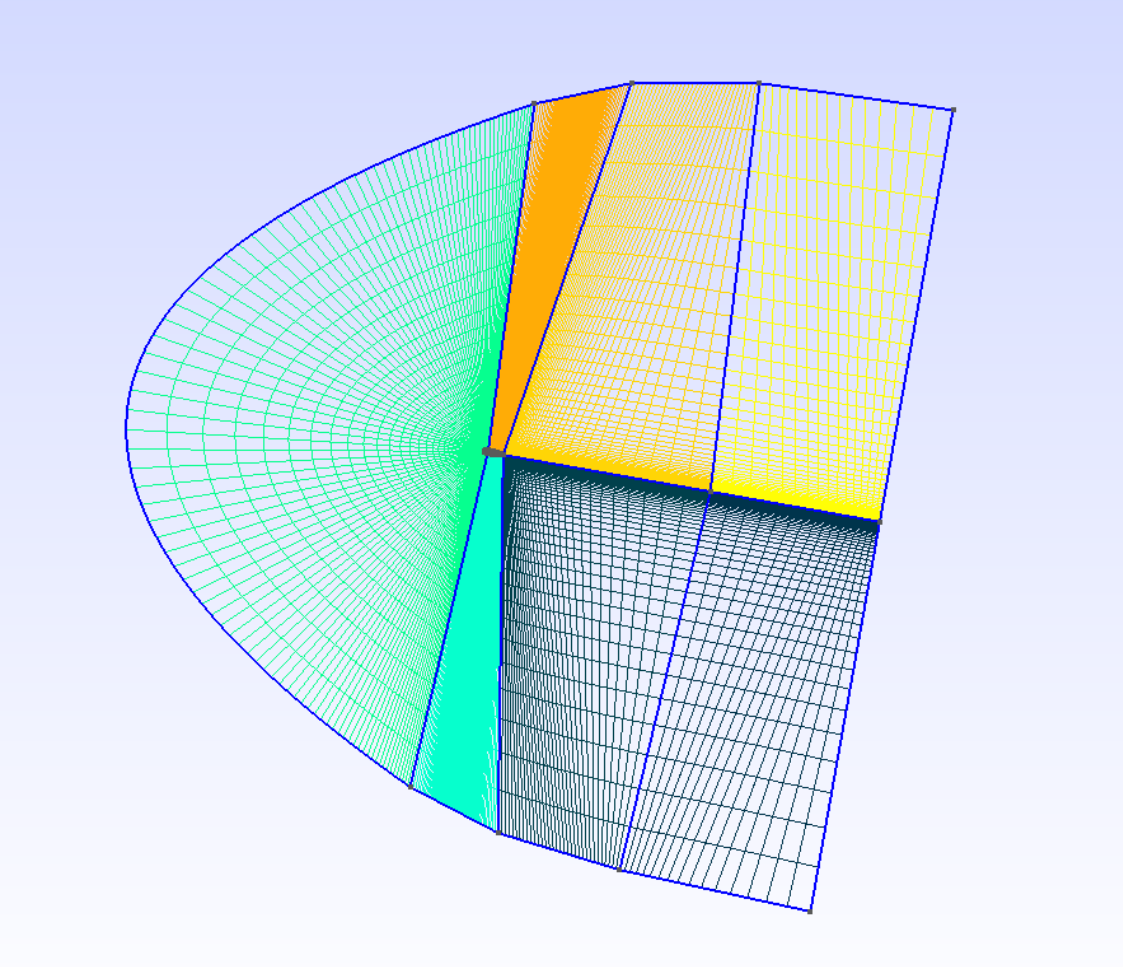

Fig. 2 Coarse Mesh

For secondary analysis, the mesh is refined, while the blocking is kept the same as the original mesh. In order to achieve a low enough y+ value, the first cell is sized to be 0.007 mm wide. This value was estimated from flat-plate boundary layer theory, using the online calculator provided by Pointwise*. This new mesh comprised of 85172 hexahedra. A similar quality check was performed on the new mesh. This new mesh had a maximum aspect ratio of 65, which was expected due to the low perpendicular size of the cells at the airfoil compared to their tangential size. This aspect ratio however was still sufficient for accurate simulations. The average angle of non-orthogonal faces increased to 20 degrees which is still acceptable. From a visual perspective, the mesh looks smooth in progression of element sizes. This new mesh is visualized Figure 3 and a closeup of the mesh around the airfoil is shown in Figure 4.

*https://www.pointwise.com/yplus

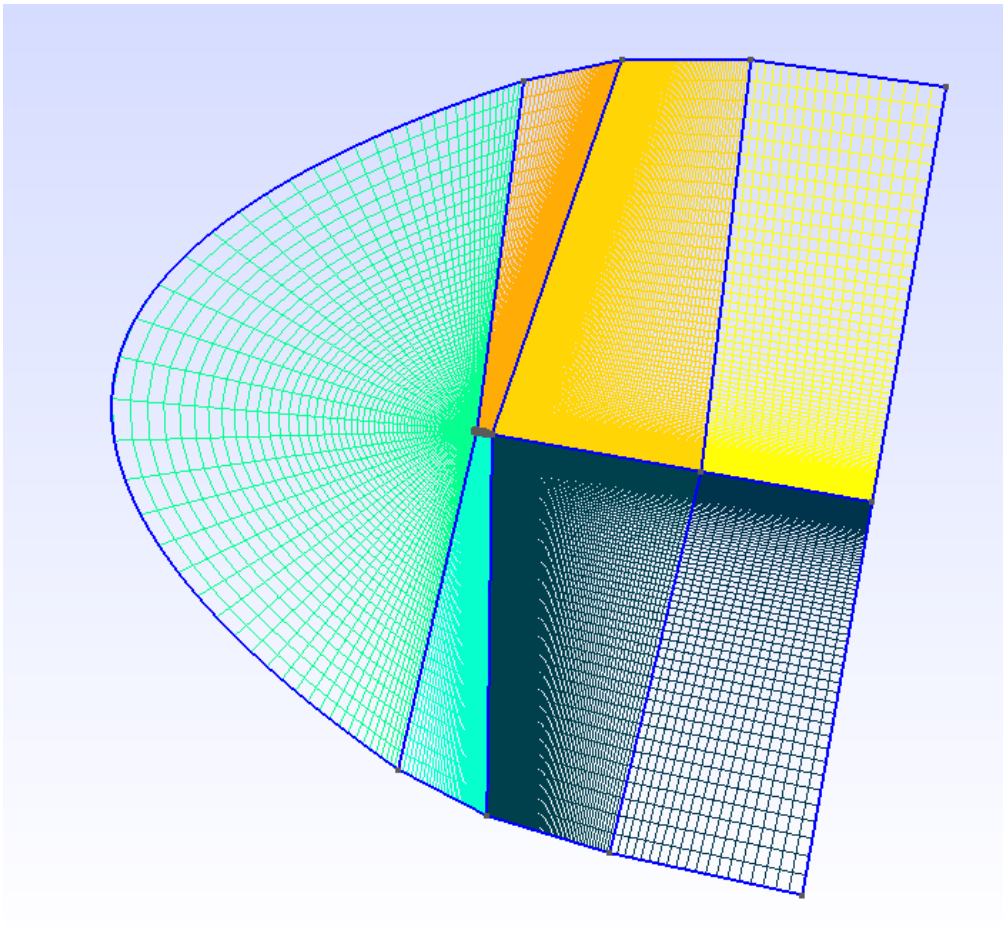

Fig. 3 Fine mesh

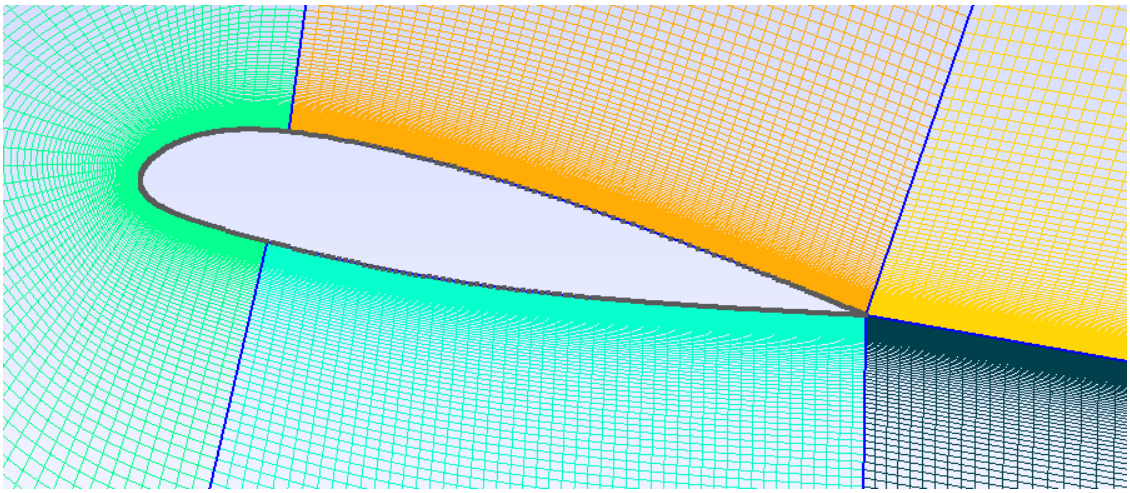

Fig. 4 Closeup of the mesh close to the airfoil

1.2. Simulation set-up

The simulation was performed using the rhoSimpleFoam solver at a Mach Number of 0.15 and a Reynolds number of 2.07 million, using the K-ω turbulence model proposed by Wilcox in 1998. The boundary conditions for pressure velocity and temperature were implemented as described in the assignment. The freestream boundary conditions for ω and k were set to a turbulence intensity of 3%, while the boundary condition for k on the airfoil was set to 0. For the boundary condition of ω on the airfoil, the approach described in [1] was used. To simulate the airfoil as a pseudo 2D case, the boundary conditions on the side were set to *empty*, to tell the solver to only solve the equations in 2 dimensions.

For spatial discretization second order accurate upwind schemes were used for convective terms, while second order central difference discretizations were used for non convective terms. In order to solve the equations a Geometric-algebraic-multigrid-solver was used. The simulation was run until a maximum residual of 10^{-5} was reached.

In order to match the prescribed Reynolds number as well as the Mach number, the total temperature was set to 294.315 K and the total pressure to 102929.865 Pa, which corresponds to a Mach Number of 0.15 an a freestream velocity of 51.4 m/s at a temperature of 293 K and a pressure of 101325 Pa. In order to match the Reynolds number of 2.07 million, the airfoil was scaled to 60.6% of its original chord.

1.3. Performed Simulations

The first simulation was performed on the coarse grid with an angle of attack of 10.1 degrees. Further simulations were carried out on the finer mesh. 3 more simulations were carried out at 10.1, 15.1 and 20.1 degrees. Another simulation was then carried out at 10.1 degrees, in which the k-ω turbulence model was changed to the k-ω SST model. A last simulation was then carried out at 10.1 degrees using first order upwind spatial discretization schemes. In order to speed up convergence of the simulations, the final result of 10.1 degrees on the fine mesh was used as the initial condition for the later simulations.

2. Results

In this section, the results of the simulations that were applied to the meshes created are presented and compared. The medium for comparison will be the visualisations of pressure and velocity distributions around the airfoil. The plots of friction and pressure coefficients will also be compared using the given reference data. Additionally, dissipation of residuals of different parameters are shown for each simulation.

2.1. Comparison between coarse and fine meshes using k-ω model

Simulations were applied to both the coarse and the fine mesh at angle of attack, α, of 10.1 degrees using the k-ω model. In the fine grid the y+ value was reduced to less than 1 everywhere on the airfoil, this improvement can be seen in Figure 5 and Figure 6. The comparison between the pressure distributions of the two are shown in Figure 7 and Figure 8. It can be said that not any obvious difference can be observed from the visuals. This conclusion can be made the same for the velocity distribution shown in Figure 9 and Figure 10.

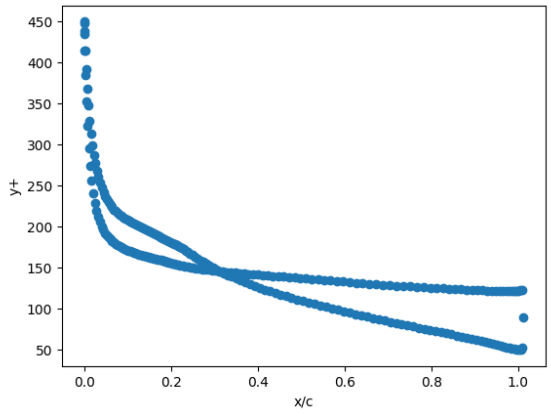

Fig. 5 y+ value on the coarse grid

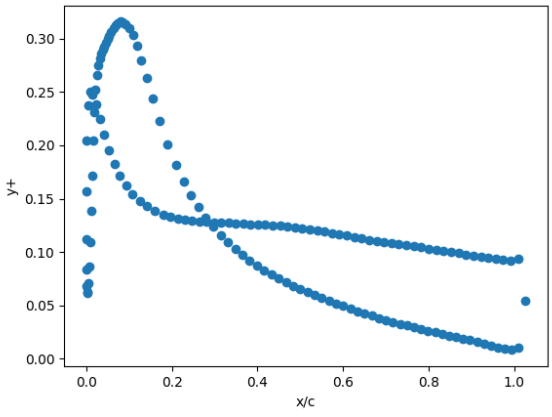

Fig. 6 y+ value on the fine grid

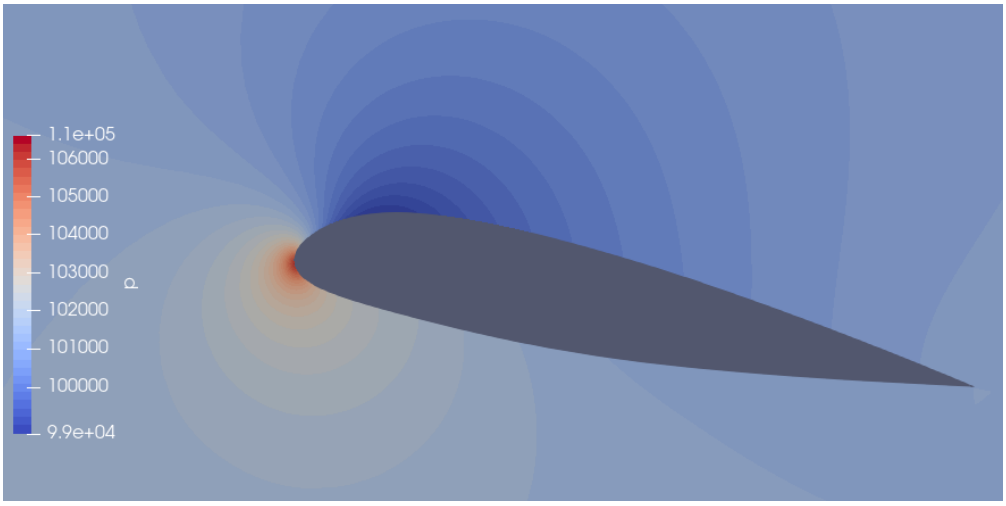

Fig. 7 Pressure distribution of coarse mesh at $\alpha = 10.1°$, k-ω model

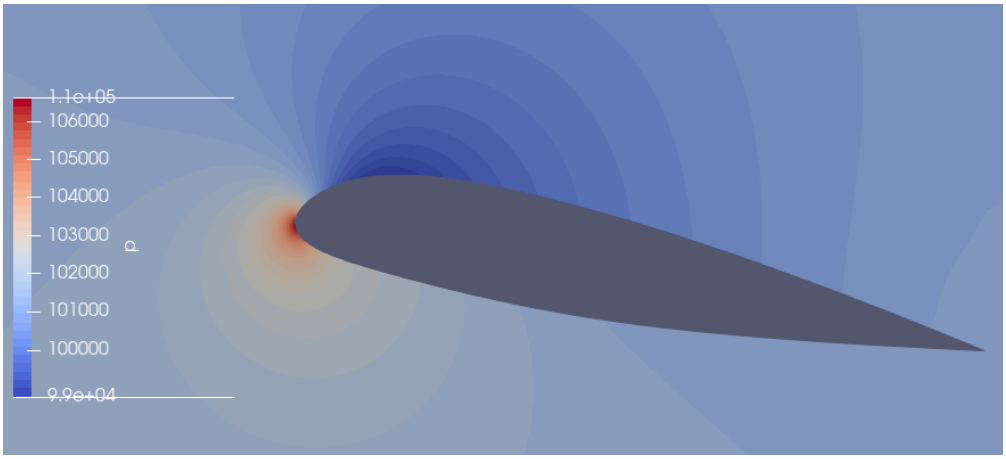

Fig. 8 Pressure distribution of fine mesh at $\alpha = 10.1°$, k-ω model

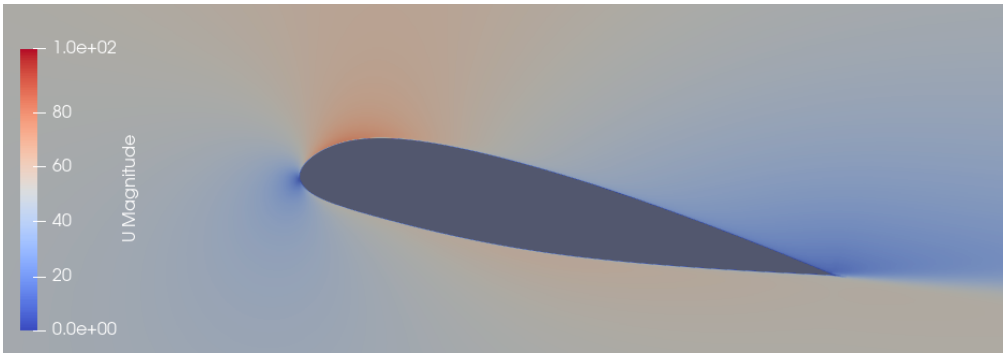

Fig. 9 Velocity distribution of coarse mesh at $\alpha = 10.1°$, k-ω model

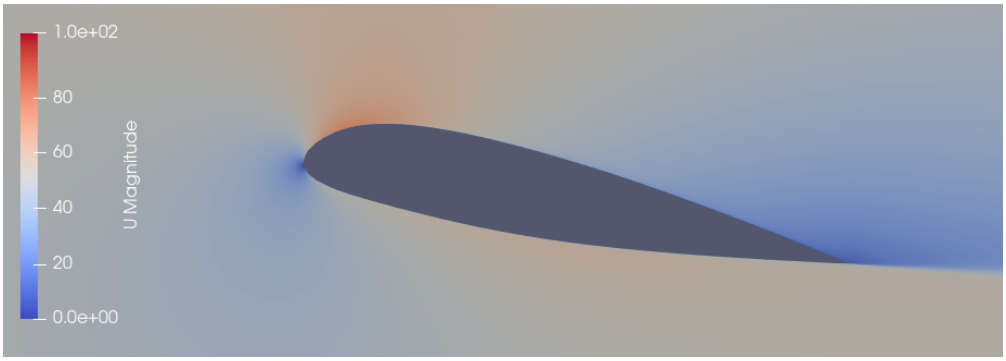

Fig. 10 Velocity distribution of fine mesh at $\alpha = 10.1°$, k-ω model

The very same can be said for the plots of friction coefficient,C_f , shown in Figure 11 and Figure 12.

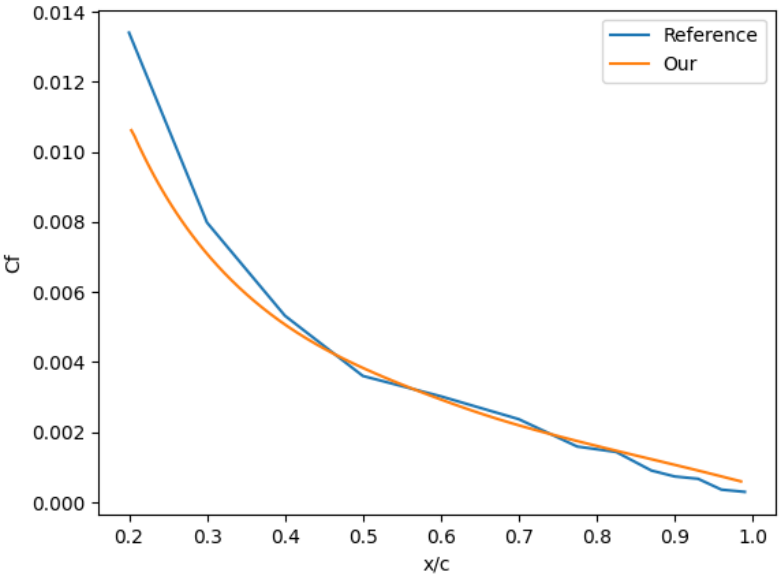

Fig. 11 C_f of coarse mesh at $\alpha = 10.1°$, k-ω model

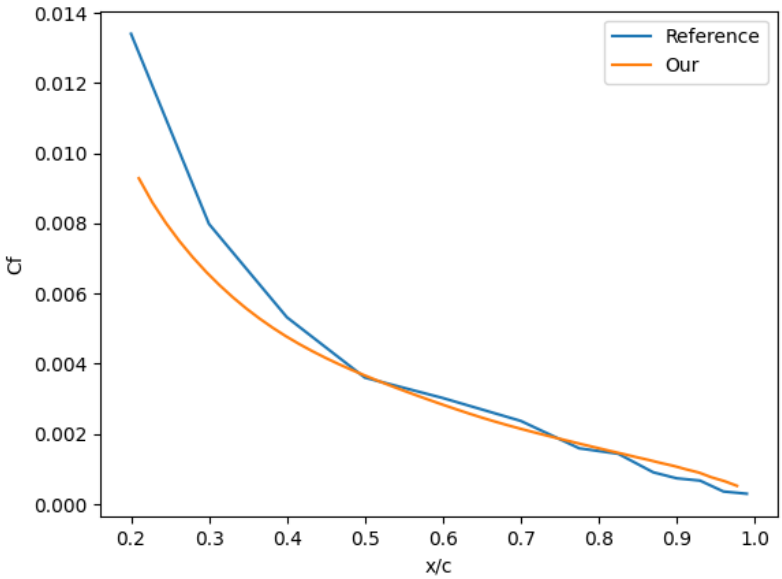

Fig. 12 C_f **of fine mesh at** $\alpha = 10.1°$**, k-**ω **model**

However for the pressure coefficient, C_p, there is a slight minor difference between the two as shown in Figure 13 and Figure 14. At the trailing edge, x/c = 1.0, C_p of the fine mesh shows a slight dip compared to the coarse mesh. Furthermore, it can be seen that the pressure coefficient exceeds 1 at the stagnation point which is clearly nonphysical behaviour.

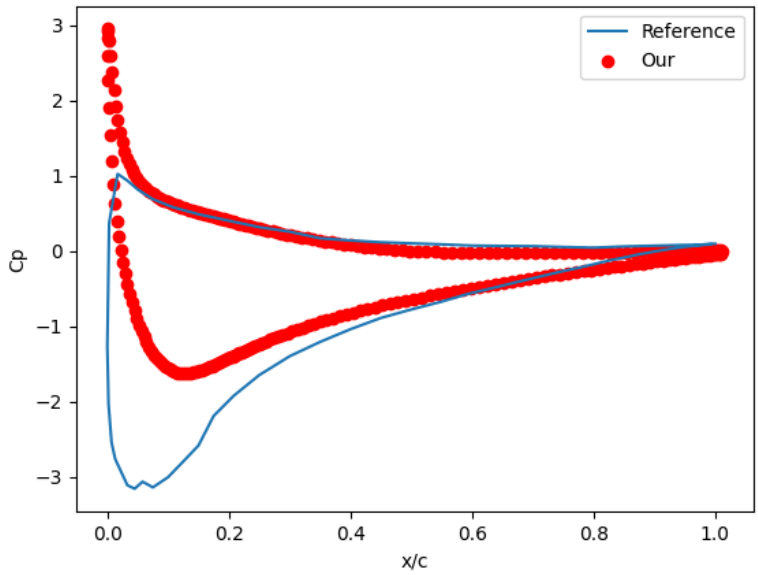

Fig. 13 C_p **of coarse mesh at** $\alpha = 10.1°$**, k-**ω **model**

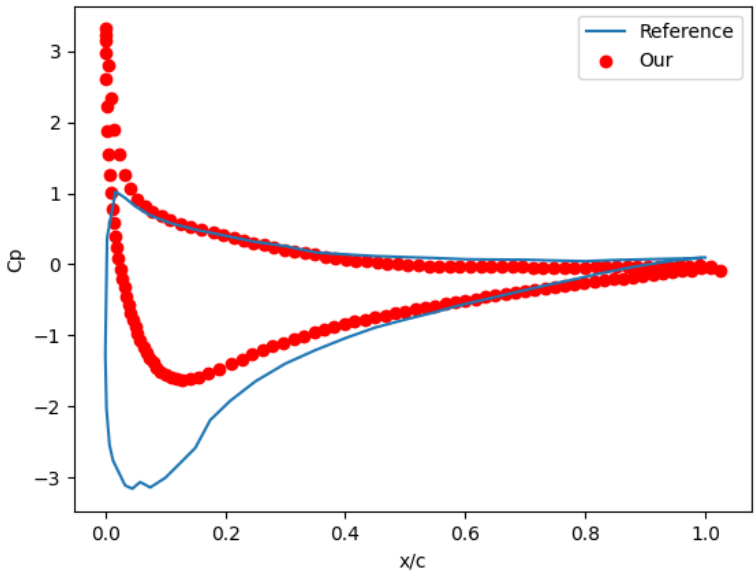

Fig. 14 C_p **of fine mesh at** $\alpha = 10.1°$**, k-**ω **model**

The convergence of the parameters in the two simulations are shown as residuals in Figure 25 and Figure 26. It can be seen that the coarse grid converges faster, which was as expected since the matrices of the finer mesh have to accommodate a much larger range of element sizes and thus having a higher spectral radius, ultimately leading to slower convergence.

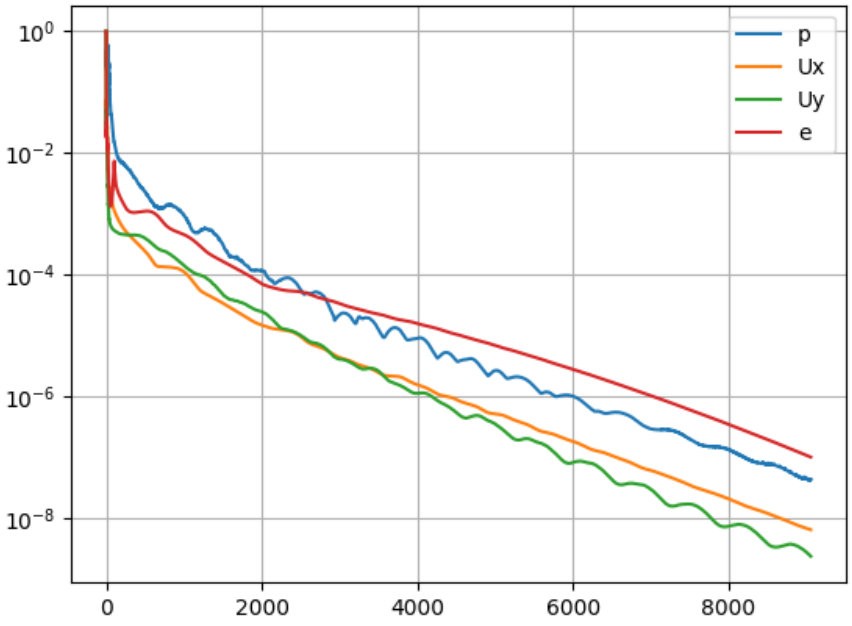

Fig. 15 Residuals of coarse mesh at $\alpha = 10.1°$, k-ω model

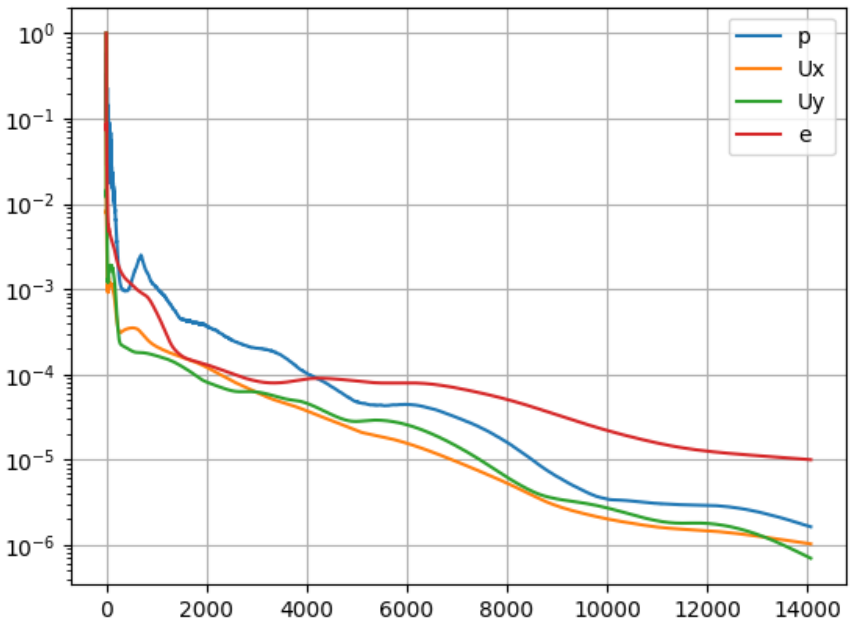

Fig. 16 Residuals of fine mesh at $\alpha = 10.1°$, k-ω model

2.2. Comparison between different angles of attack using k-ω model

Using the fine mesh, simulations were conducted for α = 10.1, 15.1, 20.1 degrees. The pressure distributions are shown in Figure 8, Figure 17 and Figure 18. Gradual changes can be observed. Similar gradual changes can be observed from the velocity distributions shown in Figure 10, Figure 19 and Figure 20.

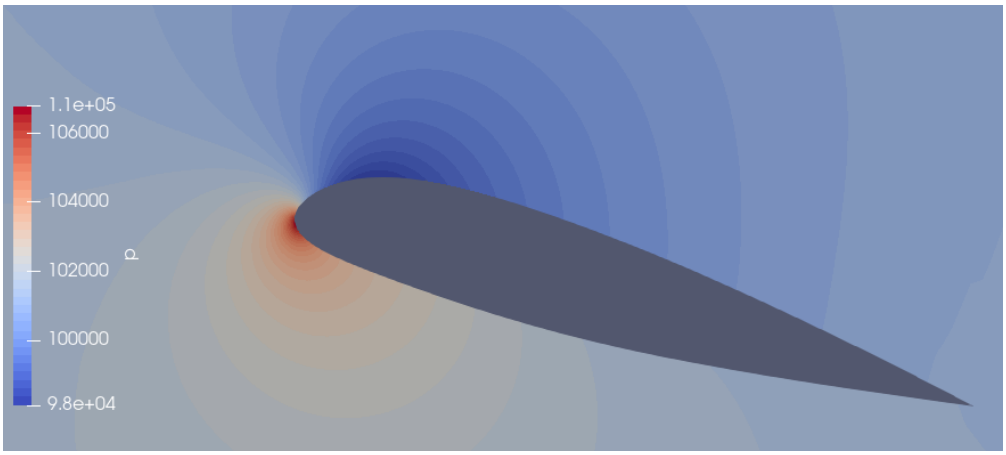

Fig. 17 Pressure distribution of fine mesh at α = 15.1°, k-ω model

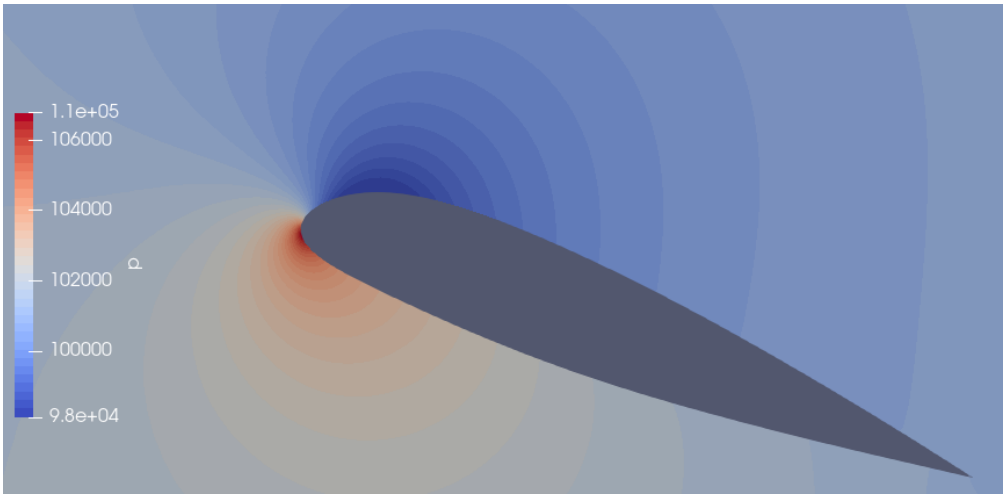

Fig. 18 Pressure distribution of fine mesh at α = 20.1°, k-ω model

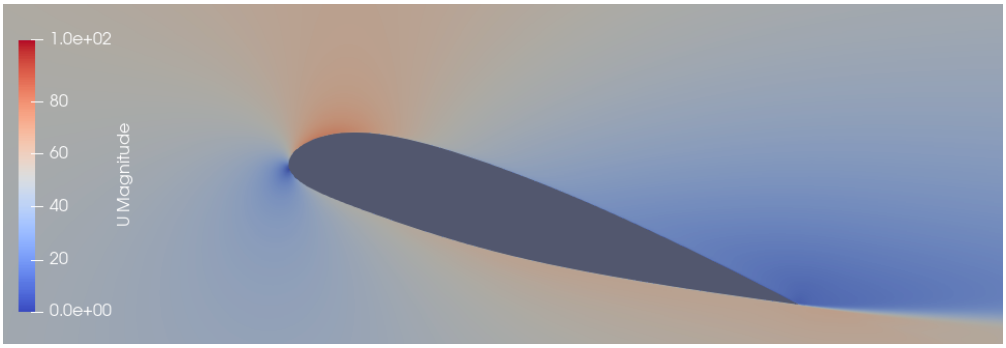

Fig. 19 Velocity distribution of fine mesh at α = 15.1°, k-ω model

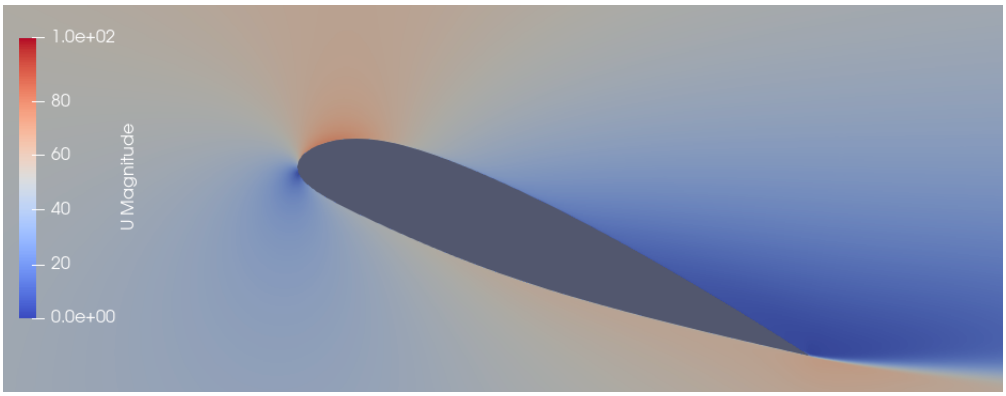

Fig. 20 Velocity distribution of fine mesh at $\alpha = 20.1°$, k-ω model

As for the friction coefficient, a large difference can be seen from $\alpha = 20.1$ shown in Figure 22 compared to the other two angles of attack in Figure 12 and Figure 21. This is due to the reference model having shown a flow separation whereas in the k-ω model, the flow stayed attached. Apart from this, for $\alpha = 15.1$, C_f does not manage to converge to the same value as the reference like how $\alpha = 10.1$ did. This could be due to k-ω model not being able to resolve the flow accurately at higher angle of attack as we have realised in the further analysis in the later stage of the assignment.

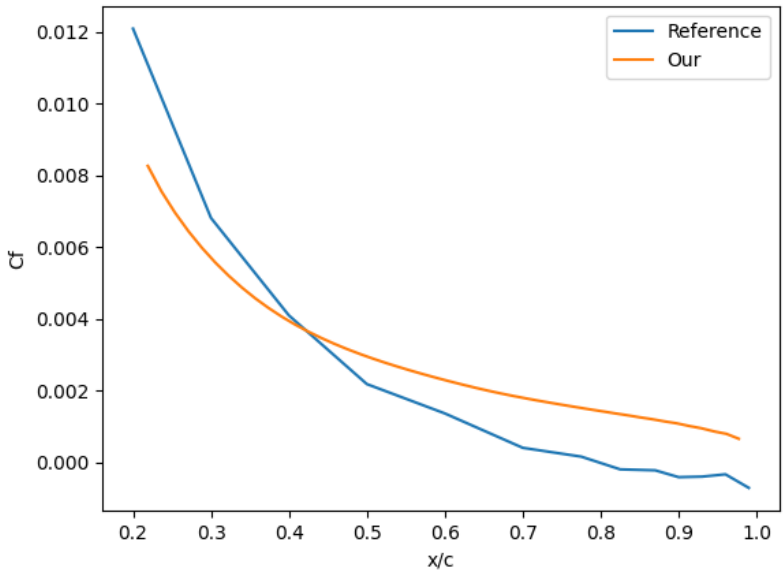

Fig. 21 C_f of fine mesh at $\alpha = 15.1°$, k-ω model

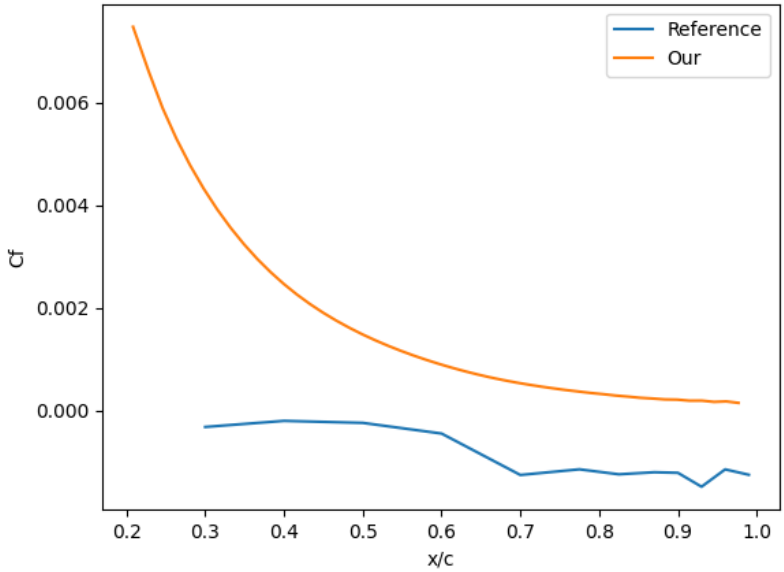

Fig. 22 C_f **of fine mesh at** $\alpha = 20.1°$**, k-**ω **model**

The shortcomings of k-ω model can also be shown in the C_p plots in Figure 14, Figure 23 and Figure 24 whereby none of the simulations was able to accurately depict the reference data.

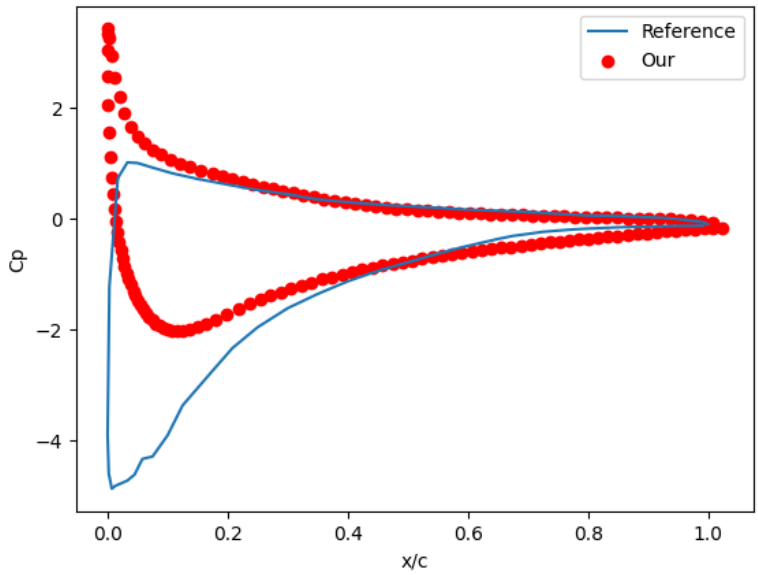

Fig. 23 C_p **of fine mesh at** $\alpha = 15.1°$**, k-**ω **model**

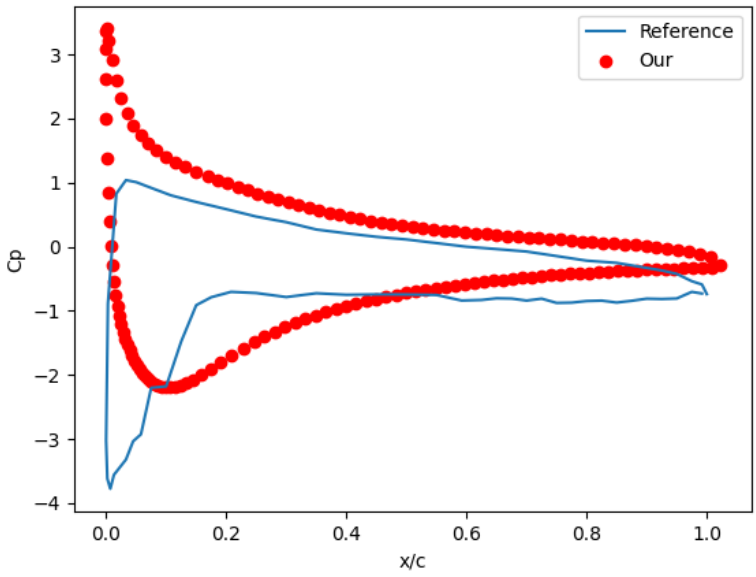

Fig. 24 C_p **of fine mesh at** $\alpha = 20.1°$**, k-**ω **model**

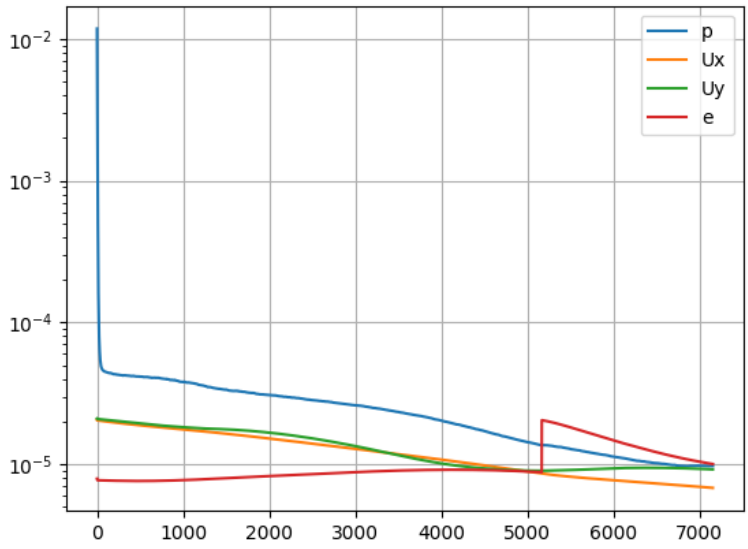

Fig. 25 Residuals of fine mesh at $\alpha = 15.1°$**, k-**ω **model**

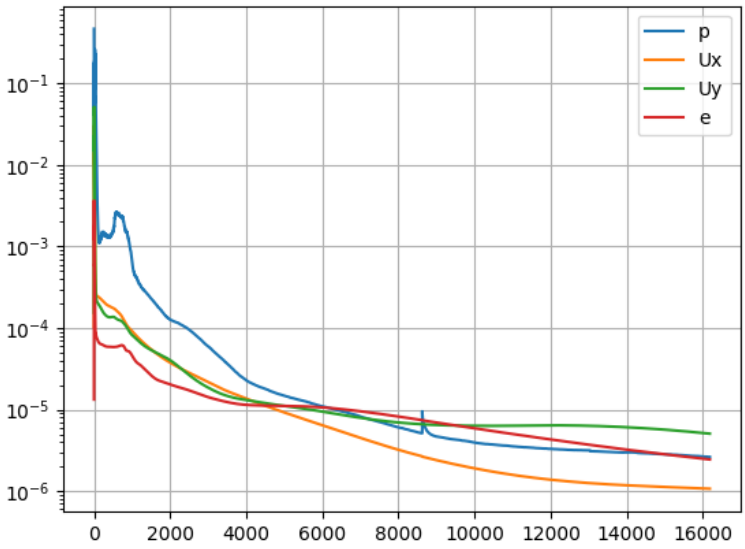

Fig. 26 Residuals of fine mesh at $\alpha = 20.1°$, k-ω model

2.3. Comparison between k-ω and $k - \omega$ SST models

In order to better account for anisotropic turbulence, a simulation using the $k - \omega$ SST was performed using the same boundary conditions and fine mesh compared to the original simulation at 10.1 degrees angle of attack. The results of the simulation can be seen in Figure 27, Figure 28, Figure 29 and Figure 30.

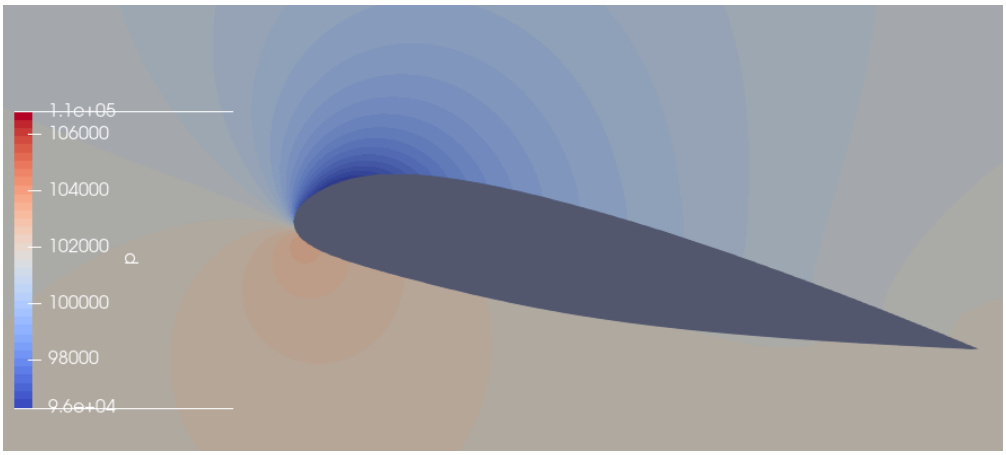

Fig. 27 Pressure distribution of fine mesh at $\alpha = 10.1°$, SST model

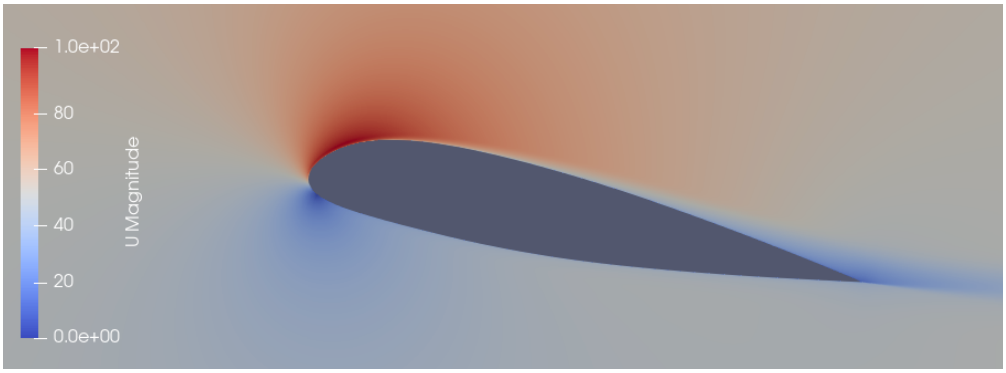

Fig. 28 Velocity distribution of fine mesh at $\alpha = 10.1°$, SST model

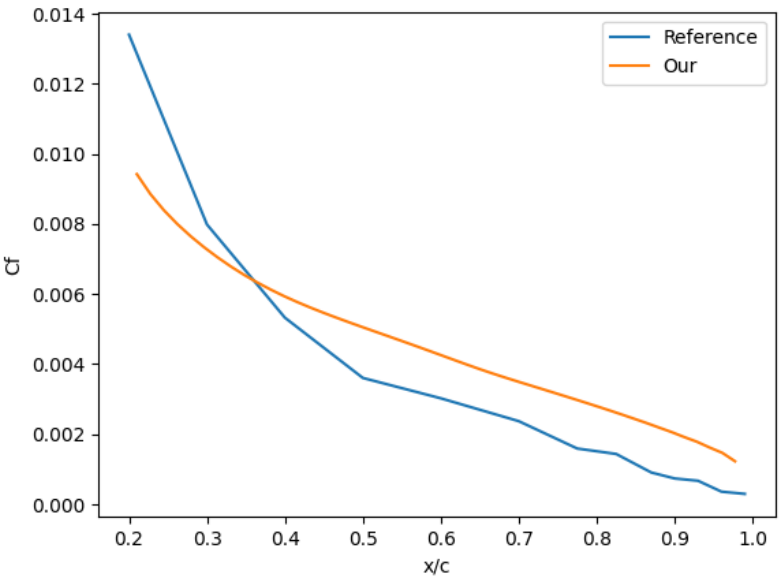

Fig. 29 C_f of fine mesh at $\alpha = 10.1°$, k-ω SST model

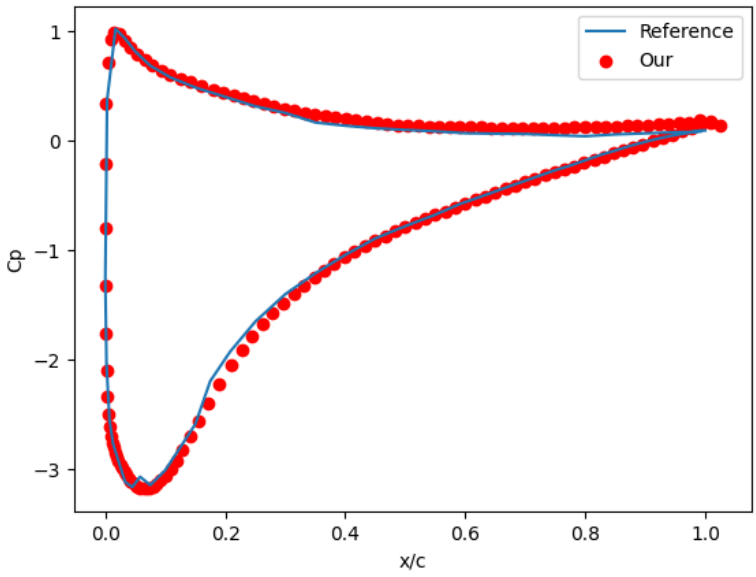

Fig. 30 C_p **of fine mesh at** $\alpha = 10.1°$**, k-**ω **SST model**

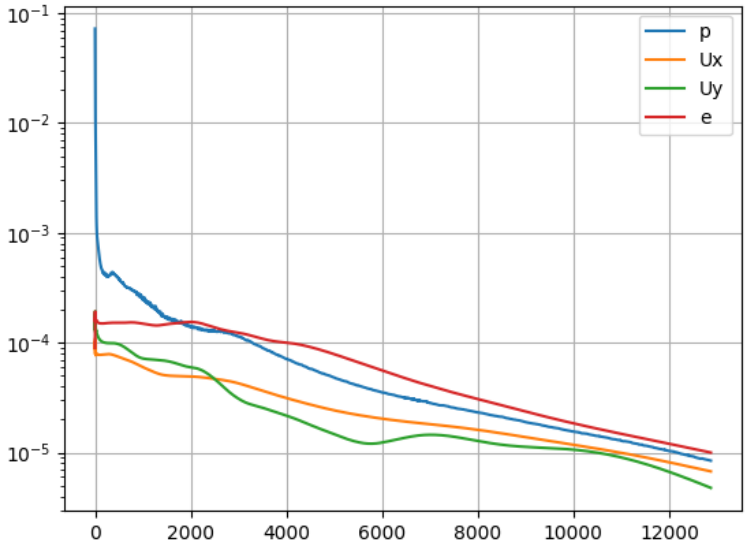

Fig. 31 Residuals of fine mesh at $\alpha = 10.1°$**, k-**ω **SST model**

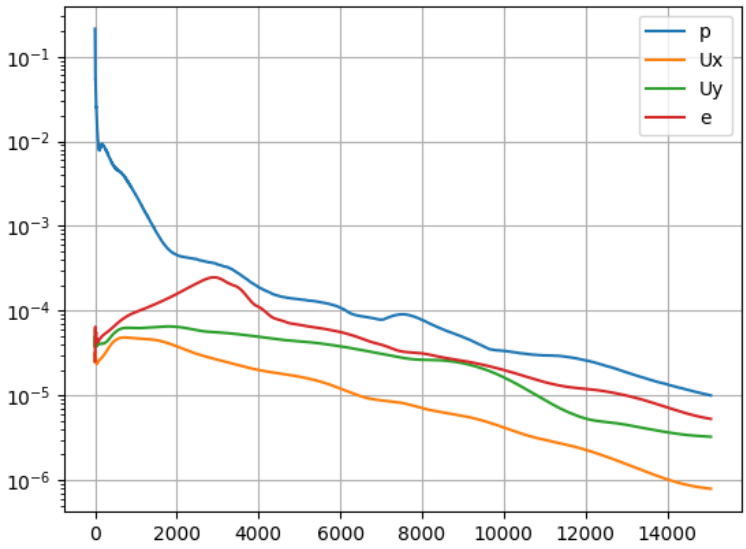

Fig. 32 Residuals of fine mesh at $\alpha = 10.1°$, first order upwind scheme

From these results it can be seen that compared to the standard $k - \omega$ model, the SST version better predicts the pressure distribution over the airfoil, given by the reference data. It however overestimates the skin friction drag especially after 40% of the chord. On a positive note, this overestimation does not propagates down the rear half of airfoil but instead is kept constant. Visually, the boundary layer development can be seen very well in the velocity distribution of the $k - \omega$ SST model compared to the previously used model.

2.4. Implementation of the first order upwind scheme

As the SST model yielded more accurate results compared to the standard model, this model was used for the following simulation. In this simulation the order of accuracy for spatial discretization was reduced to a first order upwind scheme from a second order accurate scheme. The results of this simulation can be seen in Figure 33, Figure 34, Figure 35 and Figure 36.

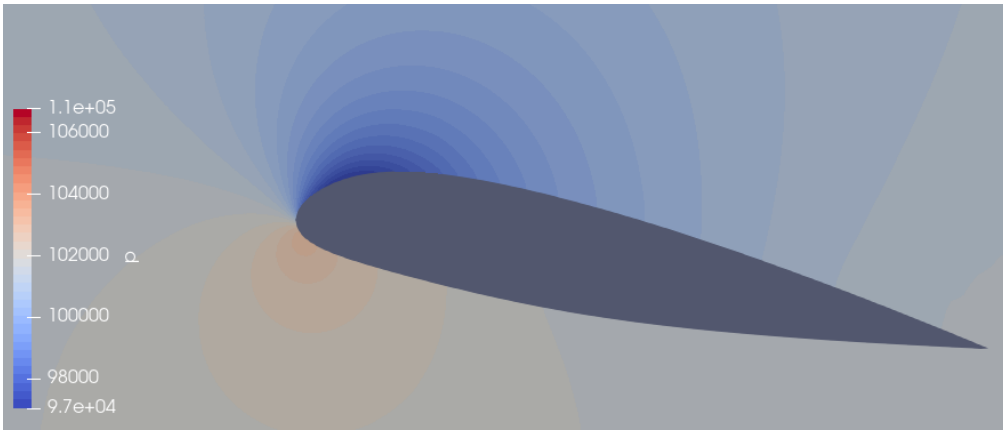

Fig. 33 Pressure distribution of fine mesh at $\alpha = 10.1°$, first order upwind scheme

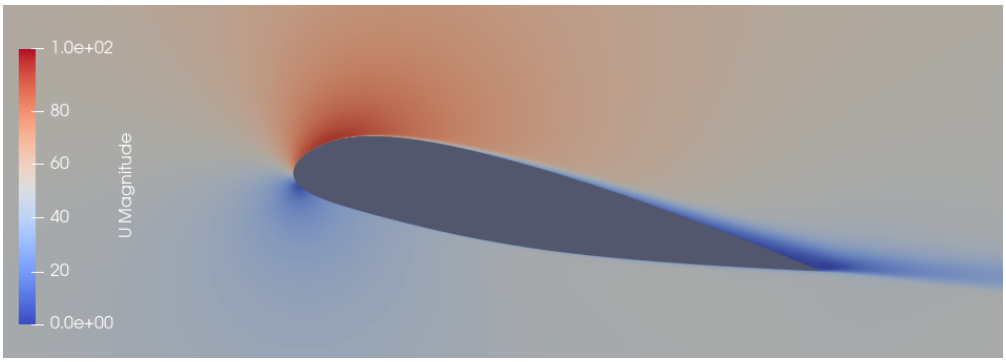

Fig. 34 Velocity distribution of fine mesh at $\alpha = 10.1°$, first order upwind scheme

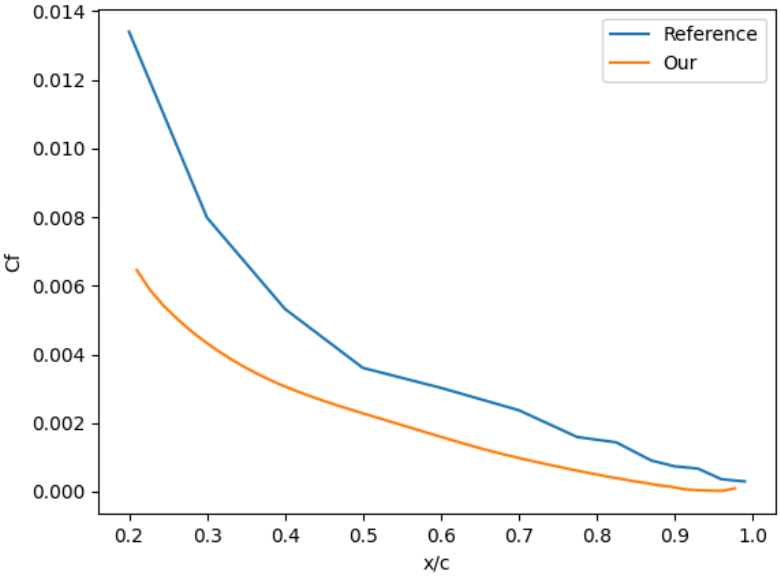

Fig. 35 C_f of fine mesh at $\alpha = 10.1°$, first order upwind scheme

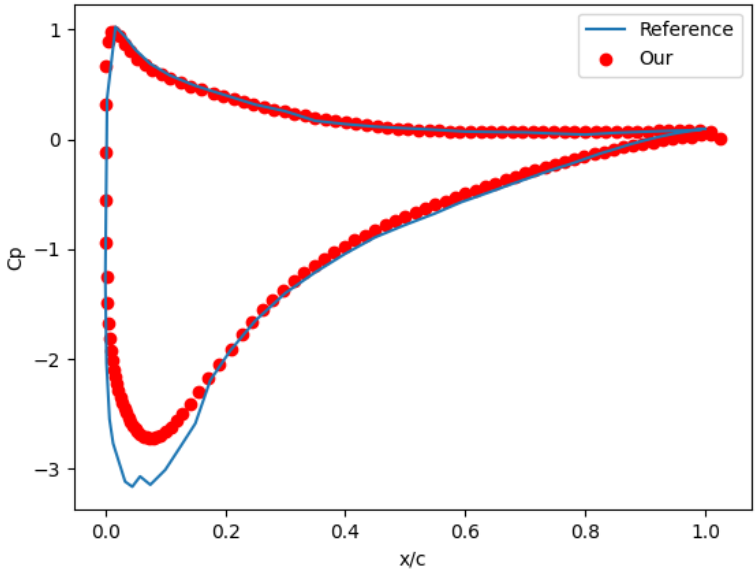

Fig. 36 C_p of fine mesh at $\alpha = 10.1°$, first order upwind scheme

It can be seen that the pressure distribution still matches the reference data approximately, however is less accurate than the the higher order discretization which is to be expected. in contrast to the higher order discretization, the skin friction coefficient is underestimated in this simulation.

Figure 37 directly compares the first and second order scheme of the SST model. It can be clearly seen at the wake that the second order scheme better resolves the wake up of the airfoil since for the first order, the velocity expands in the wake which is not an expected result whereas it dissipates for the second order.

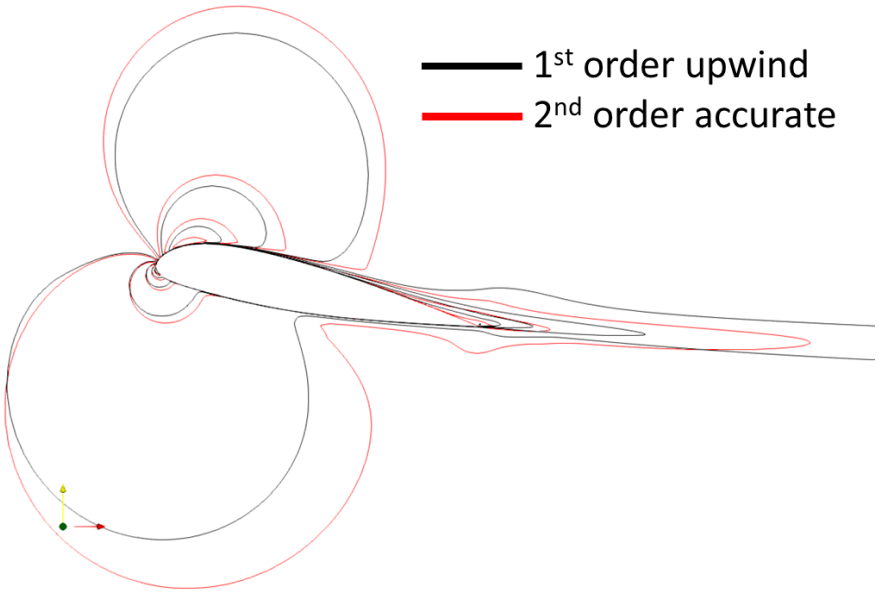

Fig. 37 Velocity distribution comparison of first order upwind and 2nd order accurate scheme

3. Conclusion and recommendations for further research

From this simulation it is suggested that the $k-\omega$ turbulence model is not suitable for predicting accurate pressure distributions over an airfoil at the tested angles of attack. The predictions for skin friction drag however were accurate and matched the reference data to a certain extent. The $k-\omega$ SST model increased accuracy of the pressure distribution significantly, while losing accuracy of the skin friction drag to a certain extent. The obtained accurate results for $k-\omega$ are however not conclusive as only about 40 % of the airfoil surface was compared to reference data. The effect of spatial discretization order is visible, however its impact is significantly lower than the chosen turbulence model. For further simulations it is recommended to not use the standard $k-\omega$ turbulence model but opt for the $k-\omega$ SST model as it yielded more accurate results for this specific case. The values for Lift and Drag coefficient can be found in Table 1. It can be seen that the standard $k-\omega$ model underestimates lift while overestimating drag when compared to the SST model.

Table 1 Lift and drag Coefficients for the different simulations

Case	C_l	C_d
Coarse mesh, k-ω, $\alpha = 10.1°$	0.844	0.279
Fine mesh, k-ω, $\alpha = 10.1°$	0.855	0.2957
Fine mesh, k-ω, $\alpha = 15.1°$	1.22	0.44
Fine mesh, k-ω, $\alpha = 20.1°$	0.8	0.3
Fine mesh, k-ω SST, $\alpha = 10.1°$	1.34	0.029
Fine mesh, k-ω SST,First order upwind, $\alpha = 10.1°$	1.165	0.058

References

[1] Menter, F., "Zonal Two Equation k-w Turbulence Models For Aerodynamic Flows," *23rd Fluid Dynamics, Plasmadynamics, and Lasers Conference*, 1993.